European Journal of Neuroscience, Vol. 26, pp. 1322–1332, 2007 doi:10.1111/j.1460-9568.2007.05735.x

Noise-improved signal detection in cat primary visual cortex via a well-balanced stochastic resonance-like procedure

Klaus Funke,[1] Nicolas J. Kerscher[1] and Florentin Wörgötter[2]
[1]Department of Neurophysiology, Medical Faculty, Ruhr-University Bochum, 44780 Bochum, Germany
[2]Department of Computational Neuroscience, University of Göttingen, 37073 Göttingen, Germany

Keywords: enhanced signal detection, eye tremor, image jitter, ROC analysis, signal-to-noise ratio, visual noise

Abstract

Adding noise to a weak signal can paradoxically improve signal detection, a process called 'stochastic resonance' (SR). In the visual system, noise might be introduced by the image jitter resulting from high-frequency eye movements, like eye microtremor and microsaccades. To test whether this kind of noise might be beneficial or detrimental for cortical signal detection, we performed single-unit recordings from area 17 of anaesthetized cats while jittering the visual stimulus in a frequency and amplitude range resembling the possible range of eye movements. We used weak, sub- and peri-threshold visual stimuli, on top of which we superimposed noise with variable jitter amplitude. In accordance with the typical SR effect, we found that small noise levels actually increased the signal-to-noise ratio (SNR) of previously weak cortical visual responses, while originally strong responses were little affected or even reduced. Above a certain noise level, the SNR dropped a little, but not as a result of increased background activity – as would be proposed by SR theory – but because of a lowered response to signal and noise. Therefore, it seems that the ascending visual pathway optimally utilizes signal detection improvement by a SR-like process, while at the same time preventing spurious noise-induced activity and keeping the SNR sufficiently high.

Introduction

The apparently paradoxical phenomenon of 'stochastic resonance' (SR) – the improved detection of weak signals when mixed with a distinct level of noise – has been demonstrated not only for physical processes but also for a couple of biological systems (for review, see Moss *et al.*, 2004). It can be observed during the transduction process at peripheral sensors, like in mechanoreceptors of crayfish (Douglass *et al.*, 1993), cricket (Levin & Miller, 1996) and rat (Collins *et al.*, 1996a), and in human muscle spindles (Cordo *et al.*, 1996) as well as for sensory perception, as demonstrated for human tactile sensations (Collins *et al.*, 1996b; Manjarrez *et al.*, 2002) and for visual perception (Simonotto *et al.*, 1997; Ditzinger *et al.*, 2000). Furthermore, as a physiologically objective measure for central processes influenced by SR, it has been shown that visually induced cortical potentials can be amplified by adding noise to the visual signal (Mori & Kai, 2002). The effect of SR is even detectable at the motor site, e.g. as an improved performance of human balance control due to enhanced mechano-sensation (Priplata *et al.*, 2002). So far, however, the SR phenomenon has not been demonstrated for central (cortical) sensory processing at the single-unit level.

In order to exhibit SR, a sensor has to be equipped with a non-linearity which, in most neuronal systems, is realized by the action potential (AP) threshold of the cell membrane. In this case, subthreshold depolarizations of the membrane potential will be pushed across the AP threshold if added noise increases the fluctuations of the membrane potential (Moss *et al.*, 2004). However, this will be beneficial only if an optimal level of noise is added to the signal as higher noise amplitudes will by themselves become supra-threshold, causing enhanced background activity leading to deterioration of signal processing in the neuronal network. At this point one may wonder whether the sensory systems of the brain are actually able to make use of SR. Recently, Greschner *et al.* (2002) demonstrated that spatio-temporal image movement with a frequency and amplitude resembling the periodic eye movements in turtles improves retinal visual signals.

The study we describe here was designed to test whether noise due to image jitter – as will be produced preferentially by high-frequency eye movements, like the microtremor or microsaccades – might be suitable to improve visual signal detection at the single-cell level in the primary visual cortex. To this end, we performed single-unit recordings from area 17 of the anaesthetized and paralysed cat, with natural eye movements eliminated by blockade of neuromuscular signal transmission while instead jittering the visual stimulus within a frequency and amplitude range covering possible eye movement parameters. In short, we found that almost every cortical neuron showed an enhanced signal-to-noise ratio (SNR) when a moderate noise level had been added to the visual stimulus. Higher noise amplitudes diminished the SNR somewhat but not, as expected, as a result of increased background activity, but via reduced responsiveness to signal and noise, thereby avoiding a further decrease in SNR. These findings demonstrate that cortical neurons are able to use the beneficial aspect of SR, but in addition are preventing themselves from being non-specifically excited by the noise.

Materials and methods

General procedures

Cats were prepared for single-unit recording in area 17 initially under ketanest (10 mg/kg)/rhompun (2 mg/kg) anaesthesia with incisions

Correspondence: Professor K. Funke, as above.
E-mail: funke@neurop.ruhr-uni-bochum.de

Received 28 March 2007, revised 6 June 2007, accepted 3 July 2007

and pressure points additionally anaesthetized with xylocain (2%, Astra Chemicals, Germany). For details of surgery, see Moliadze *et al.* (2005). Anaesthesia was continued by artificial respiration with a mixture of N_2O/O_2 (70 : 30) and halothane (0.6–2.0 Vol.-%). The halothane level was adapted to the experimental situation, with 0.6% during the recording sessions that followed surgery by hours and lasted up to 7 days, and with 2.0% during any potentially noxious procedure like handling the contact lenses or penetrating the dura mater. The halothane level was also raised when electroencephalogram (EEG) showed signs of becoming desynchronized, in order to maintain sufficient narcosis. Immobilization of the animal was achieved by alcuronium chloride infusion via the femoral artery (Alloferin, 0.15 mg/kg/h dissolved in 5% sucrose–Ringer's solution) and the aid of a stereotaxic frame. Blood pressure, heart rate, respiratory CO_2 and O_2 levels, body temperature and the EEG were continuously monitored to control and maintain the physiological state of the animal. All experimental procedures were approved by the German government (50.8735.1 no. 29.8, 81.6 and 105/7) and by the University Animal Welfare Committees, and also conformed to the directives of the European Community Council (86-609-EEC) and the guidelines of animal welfare laws in Germany, UK and the USA.

Stimulus display and recording

Bar stimuli (3.0×0.25 deg) were generated by a modified slide projector (Kindermann Universal, Germany) and projected via a galvanic mirror system (SSA 3001, MOT GmbH, Germany) onto a tangent screen (with 1 cd/m^2 background illumination) 114 cm in front of the cat's eyes with optimal orientation with regard to receptive field preference. The optics of the eyes were corrected by spectacle lenses for this viewing distance. An array of 5×5 high-power, green light-emitting diodes (LED) was used as the light source. LEDs were chosen to enable fast, computer-controlled brightness modulations within the range of 1–8 cd/m^2 (measured on screen). Sinusoidal motion of the stimulus (up to 3.15 deg) and broad-band jitter of the stimulus (random noise of 1–200 Hz of equal power at up to 2 deg standard deviation, σ) were generated by controlling the mirror system with Spike2 software via the computer interface CED 1401 plus (Cambridge Electronic Design, UK). Noise was realized by jittering the bar stimulus in one dimension, perpendicular to its long edge and corresponding to the directions of bar motion. Spike times, analogue EEG signal and the feedback outputs of the mirror system (to achieve adaptively equal power for all tremor frequencies) were recorded in parallel with the same system. APs were extracellularly recorded from area 17 with varnished tungsten electrodes (about 1 MOhm, FHC, ME, USA). Spikes were separated from noise via a two-step process of non-linear amplification and threshold detection (Osaka *et al.*, 1988).

Test procedures

To systematically test the effect of noise amplitude on visual responses, six different noise levels (0 as control and five different levels of up to a standard deviation [σ] of 2 deg for testing) were combined with three different amplitudes of the test stimulus – one sub- to peri-threshold, the second slightly supra-threshold and the third eliciting a stronger response. Amplitude relates either to bar motion (sinusoidal motion of up to 3.15 deg) or brightness modulation of a stationary bar between 1 and 8 cd/m^2. In case of bar motion, increasing motion amplitude proportionally increased also the speed of motion. One motion or brightness cycle had a length of 500 ms, and 10 cycles were presented consecutively (2 Hz), resulting in a sweep length of 5000 ms. In addition, measurements were performed without modulation of the test stimulus (constant position and brightness), but with one of the six test noise levels. These 24 different stimulus situations were presented in an interleaved manner to minimize effects related to response variability, e.g. changes in EEG state (Li *et al.*, 1999). For reasons of better distinction from other possible noise sources, we will call the spatial noise (jitter) 'stimulus tremor' throughout the article.

Prior to each set of measurements, the position and spatial structure of the receptive field (number and size of on-subfields) were tested with an optimally orientated, slowly moving bar, and also with bars randomly flashed at 16 different positions across the whole receptive field. Then, the most responsive region was chosen as the centre position for the test stimulus. Receptive fields of all cells were within 3–7 deg inferior to the centre of the visual field. The width of individual subfields was estimated from the region showing evoked activity twice the standard deviation of background activity. Data of simple and complex cells were pooled as no principal difference was expected for a process supposed to be of primarily peripheral (retinal) action.

Data analysis

For each combination of test stimulus and stimulus tremor amplitude, spike activity was analysed with the aid of peri-stimulus time histograms (PSTH), auto-correlation functions (ACF) and the integral of total activity (spike count). The ACF was used to calculate the SNR for visual responses. The SNR was determined by a standard method as the square of the summed response peaks in the ACF at stimulus periodicity (500 ms, corresponding to sinusoidal bar motion and brightness modulation at 2 Hz) and its integer multiples up to 5000 ms, divided by the spike-rate variance σ with regard to stimulus cycle and with time count normalized to 1 ms bins by t_u.

$$\mathrm{SNR} = \frac{1}{\sigma}\sum_{i=0}^{10}[\mathrm{ACF}(500\ i\ t_u)]^2$$

Thus, the SNR reflects how many spikes are located at the expected response peaks in relation to those outside. In addition, we applied classical signal detection theory by comparing the spike activity distributions for spontaneous and visually induced activity. The receiver operator characteristics (ROC) method was used to achieve a quantitative measure of signal detectability by the area under the ROC curve (AuROC). The latter was calculated for stimulus presentations without noise and for the added stimulus tremor amplitudes. For further details of data analysis, see figure legends.

Results

Visual cortex neurons show SR-like behaviour

To visually stimulate the neurons of cat area 17, an optimally orientated bright bar was either moved across the receptive field in a sinusoidal fashion or it was sinusoidally modulated in brightness while remaining stationary within the most responsive region of the receptive field (2 Hz test stimulus). As exemplified in Fig. 1, for a bar moving in one direction across the receptive field, visual stimuli of different strengths (motion amplitude and speed) were then combined with different noise levels (tremor amplitude, *T*). Figure 1

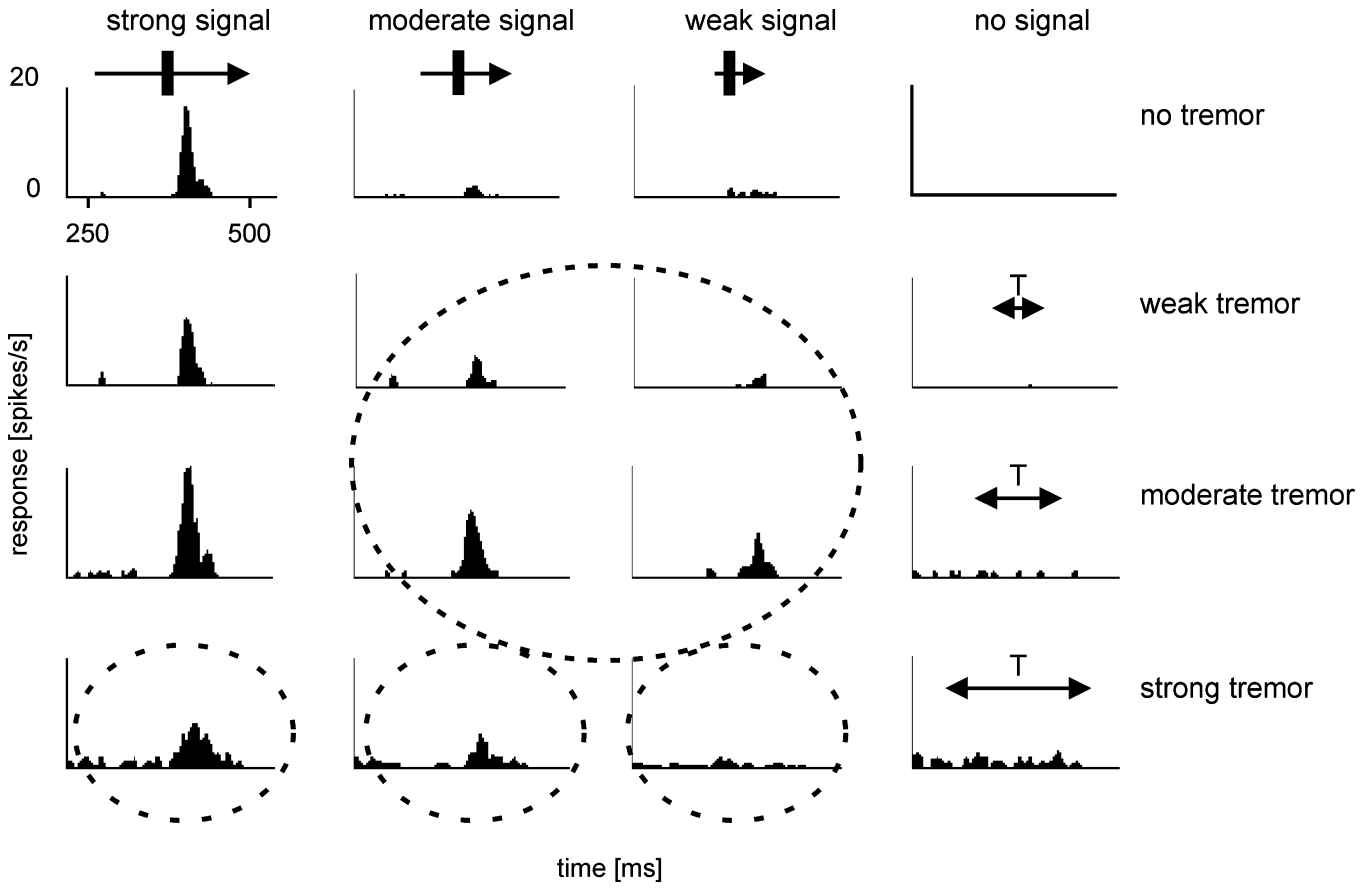

FIG. 1. Visual responses elicited by different combinations of bar motion amplitude and stimulus tremor amplitude. PSTHs show the averaged visual responses for 200 repetitions of the same combination of bar motion and stimulus tremor. Here, only responses to bar motion in the preferred direction are shown. The example shows a typical SR effect, with visual responses enhanced by low to moderate noise (tremor amplitude, large dashed circle), but somewhat decreasing responses with strong tremor (three small dashed circles). In addition to the combination of bar motion with tremor, also cases with no bar motion amplitude (right column) or no tremor (upper row) were tested. The receptive field diameter of this cell was about 0.5 deg (short axis of on-subfield). Motion amplitudes were (from strong to weak signal): 2.28, 1.14 and 0.57 deg. Tremor amplitudes were (from strong to weak): 1.28, 0.32 and 0.16 deg (arrows are not scaled for absolute amplitude).

shows typical aspects of SR: weak, sub- to peri-threshold visual responses are increased if low or moderate tremor had been added to the moving bar (pointed out by the large dashed circle). The three smaller circles indicate cases in which stronger tremor has led to a different effect, namely a decrease in response amplitude. However, the decline in the response to the sinusoidal motion happened without a considerable increase in background activity, as could be expected from supra-threshold noise components. The three diagrams to the right show that pure tremor (zero sinusoidal bar motion amplitude) also causes very little background activity even if the tremor amplitude is large. Figure 2 shows two further representative examples with visual responses analysed for different motion amplitudes (Fig. 2A) or brightness modulation depths (Fig. 2B; both with a periodicity of 2 Hz) combined with different amplitudes of stimulus tremor. In both cells, an increase of the visual response amplitude can be obtained with moderate noise levels. The corresponding peak responses as determined by the PSTH are plotted in (Fig. 2C) and (Fig. 2D) vs the standard deviation of stimulus tremor amplitude (σ) for these two cells. Interestingly, and in accordance with the hypothesis of SR, a higher amplitude of stimulus tremor is needed to increase the responses to the weakest stimuli, while a lower amplitude of tremor is sufficient for stronger – albeit still relatively weak – test stimuli (see location of peaks in Fig. 2C and D). The absolute amplitude of stimulus tremor needed to achieve response improvement varies not only with the strength of the test stimulus amplitude (motion or brightness) but also from cell to cell, and may be related to the spatial properties of the receptive fields (see below). A reduction of response amplitude accompanied by a slight broadening of the activity is found for higher stimulus tremor amplitudes, and the responses start to decline, but background activity remains low.

Quantification of SR-related changes in visual activity

In total, 79 cells recorded from seven cats were tested with bar motion and 37 cells with brightness modulation. A quantitative analysis could be performed only for 37 and 23 cells, respectively, because we rigorously excluded all cells that showed response fluctuations to constant stimulus situations over time, which may be related to state changes (Ikeda & Wright, 1974) or changes in receptive field position indicative of slow eye drifts. This conservative procedure was adopted in order to clearly distinguish the subtle SR effects from possibly arising spurious activity changes. For a reliable quantification of the visual responses, the SNR was calculated from the ACF (see Materials and methods). The first four diagrams of Fig. 3A–D show the SNR for responses to moving bars

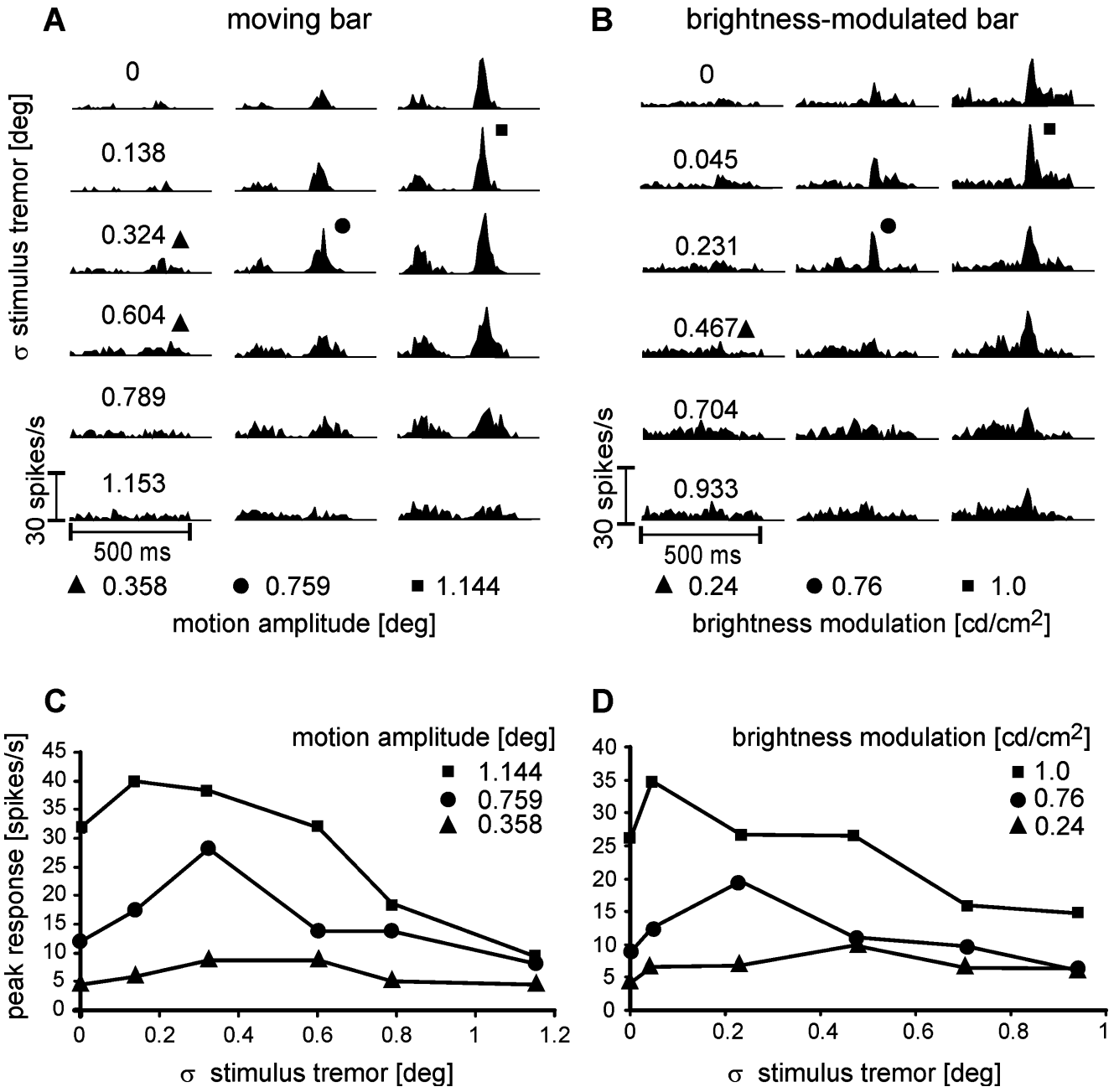

FIG. 2. Visual responses of two cells elicited by different combinations of test stimuli and stimulus tremor amplitude. The test stimulus was either a bright bar moved across the receptive field in a sinusoidal fashion at 2 Hz with three different motion amplitudes (A), or a stationary bar sinusoidally modulated in brightness at 2 Hz with three different modulation amplitudes (B). The upper rows show responses without tremor (0, controls), the rows below show responses to different stimulus tremor amplitudes added to the test stimulus. Tremor is given as standard deviation (σ) of spatial displacement. (C and D) Response peak values for the responses to different motion (A) or brightness modulation (B) amplitudes of the two cells are plotted as a function of tremor amplitude (σ). Responses to stronger test stimuli show maximal responses at lower tremor amplitudes than responses to weaker stimuli. Corresponding peak amplitudes are labelled by the symbols in (A) and (B). The receptive field size (length of short on-subfield axis) is 0.31 deg in (A) and 0.46 deg in (B). Each PSTH shows the averaged visual responses for 200 identical stimulus repetitions.

(Fig. 3A and C) and to bars modulated in brightness (Fig. 3B and D) as a function of stimulus tremor. In general, two cases could be distinguished: cells showing an increase in SNR up to a certain noise level and then a decline in SNR; and cells with a continuously declining SNR at increasing noise level. In the upper diagrams of Fig. 3A and B, we plotted all curves that showed a discrete maximum of SNR that is higher than the control response. In many cases the maxima were rather small, as expected from a typical SR effect. In general, curves with a maximum could be obtained when both the initial cell responses and the noise levels were weak. In the insets (Fig. 3A and B), curves were rearranged according to the position of their maximum in order to show that smaller, broader maxima normally are observed at higher noise levels. As we will quantify below (Fig. 4), this happens when the control responses of the corresponding cell (without noise) were rather small.

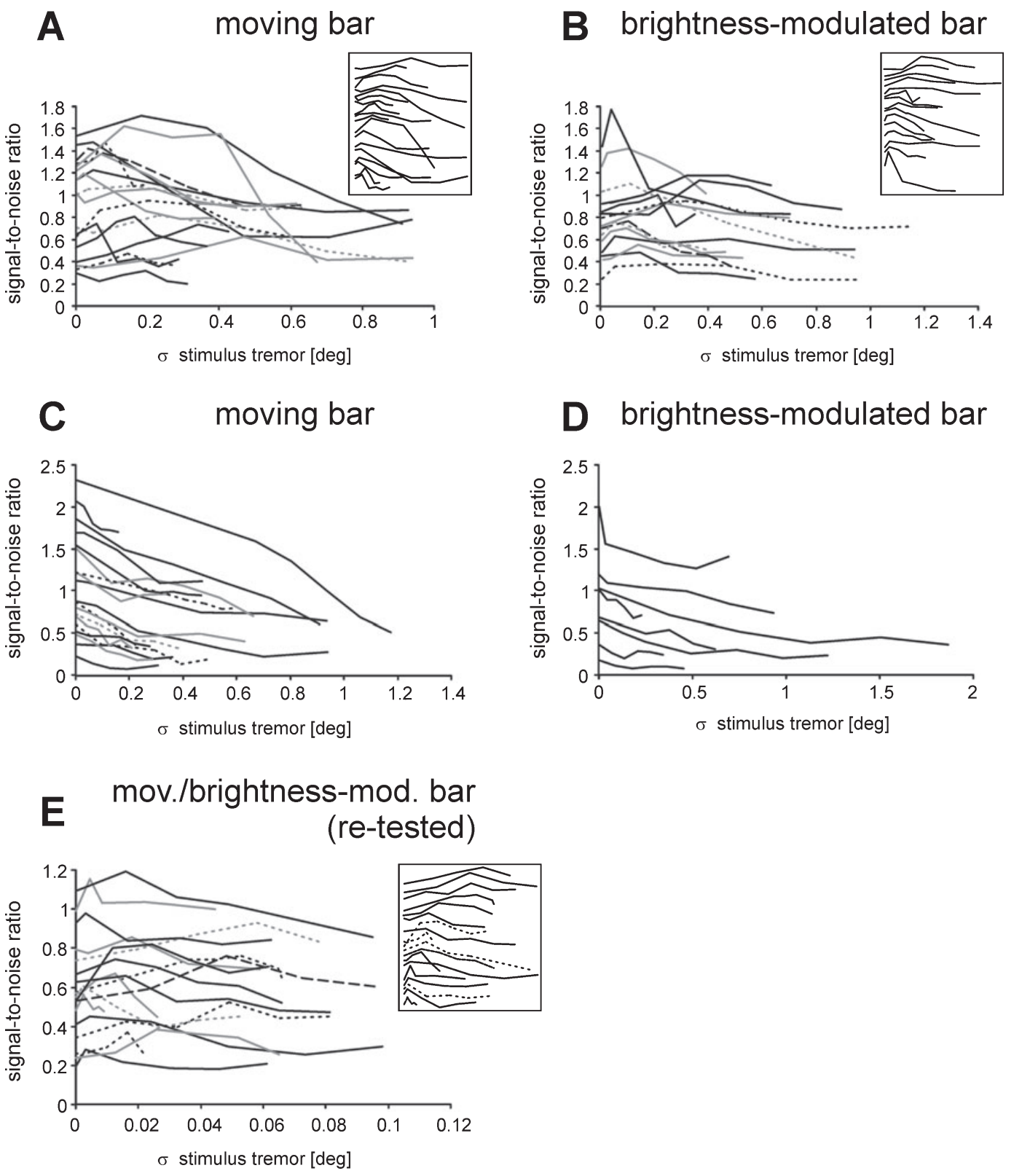

FIG. 3. Relationship between SNR of visual responses and stimulus tremor amplitude. For 37 cells tested with a moving bar, (A) and (C) show the SNR of visual responses as a function of the stimulus tremor amplitude. (A) Curves showing a discrete peak, (C) curves without a peak but a steady decline. (B and D) SNR of visual responses evoked by a bar modulated in brightness as a function of the stimulus tremor amplitude for 23 cells. (E) Another set of curves with the SNR plotted vs a lower range of stimulus tremor (one order of magnitude lower than in A–D). Data were obtained from 18 cells showing originally a decline in SNR to moving bars ($n = 13$, solid lines) and brightness-modulated bars ($n = 5$, dashed lines) at the higher tremor range used in (C) and (D). These curves now also show discrete peaks, but the increase in SNR is smaller compared with those in (A) and (B). Curves refer to only one of the three stimulus amplitudes tested for bar motion and brightness modulation (peri- or little supra-threshold stimulus). Insets in (A), (B) and (E) show the same curves as in the main diagrams, but rearranged vertically by their peak location to emphasize that peaks at low tremor amplitude are mostly sharper than peaks found at higher tremor amplitude.

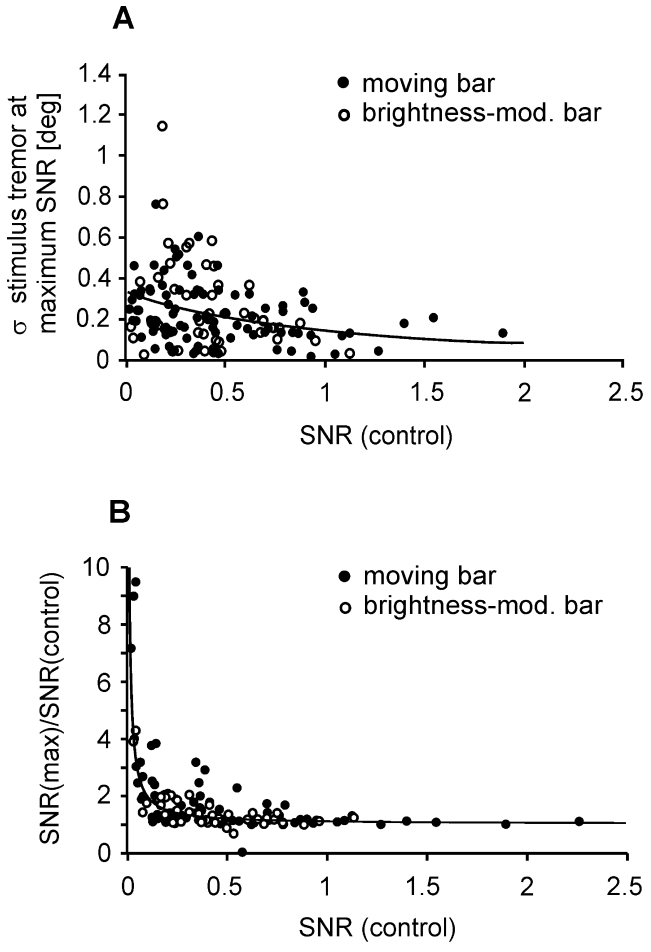

FIG. 4. Relationship of effective stimulus tremor level and increase in signal-to-noise ratio (SNR) to the strength of control responses. (A) Stimulus tremor (standard deviation, σ) yielding maximal SNR plotted as a function of control SNR. Data relate to the same cells for which SNR to noise–amplitude curves are shown in Fig. 3, but including all the three different motion amplitudes (filled dots, tested in 37 cells) and the three different brightness modulation amplitudes tested (circles, 23 cells). The distribution of data points and the fit indicate a more or less inverse relationship between strength of control responses and noise level needed to achieve response facilitation. Data points are fitted with a polynomial quadratic function [$f(x) = P1*x^2 + P2*x + P3$], $r^2 = 0.089$, not significant ($P = 0.17$). (B) Relative increase in SNR [$SNR_{(max)}/SNR_{(control)}$] plotted vs control SNR for the same data set as in (A). This data point distribution could be fitted with the function: $y = 1 + \exp(-2.3484 * x\text{^}(-1.0155))$, $r^2 = 0.69$, $P < 0.05$.

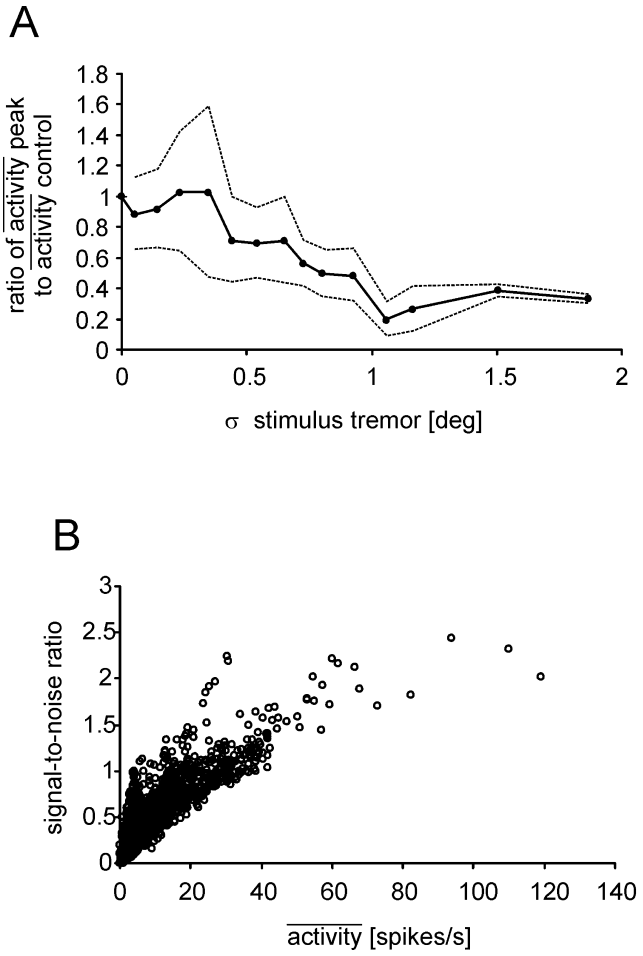

FIG. 5. Relationship between mean rate of activity and stimulus tremor amplitude, as well as SNR. (A) The curves give the grand average (solid line) and standard deviation (dashed lines) of mean activity rate for all cells tested with bar motion or brightness modulation ($n = 37 + 23$). Prior to averaging, data of individual cells were normalized to the activity during the control condition without added noise. The mean activity refers to the averaged total spike activity (integral of activity of single PSTHs as shown in Fig. 2) obtained under conditions of added noise irrespective of the general noise effect (peak at a certain noise level or steady decline of activity). Unexpectedly, the mean rate of activity declines with high noise levels. (B) SNR plotted as a function of mean activity rate for all the 1440 recordings obtained from the 24 different stimulus conditions tested in the 60 cells. SNR increased with activity, indicating that mean activity was largely related to stimulus-driven activity.

Curves in parts (Fig. 4C and D) of this figure, on the other hand, show a steady decline, indicating that increasing stimulus tremor had progressively weakened the SNR in these cases. These cells may not show an SR effect at all, but it is also possible that the stimulus conditions were not appropriate: a discrete SNR maximum may be missed if the range of noise amplitude ($\sigma = 0.1$–1 deg) had been too large. Therefore, we retested these cells with a smaller stimulus tremor range of $\sigma = 0.01$–0.1 deg. Eighteen of the 27 cells showing declining SNR curves with moving ($n = 19$) and brightness-modulated bars ($n = 8$) could be retested with the smaller stimulus tremor range and indeed now all showed a small but discrete SNR maximum with noise added (Fig. 3E, 13 with motion, five with brightness modulation), indicating that SR effects are strongly stimulus dependent, as expected. This indicates that SR can obviously be found in almost all cells of cat primary visual cortex when choosing the right stimulus conditions.

Relationship between noise level and SNR improvement

As mentioned above, we had observed that the optimal stimulus tremor amplitude for the SR effect appears to depend on the response amplitude itself. Figure 4A quantifies this aspect by plotting the stimulus tremor amplitude that led to the greatest improvement of the SNR (at the peaks of the curves in Fig. 3A, B and E) vs the response amplitude (SNR) of the control responses without stimulus tremor. Figure 4B shows also that the relative increase in SNR ($SNR_{(max)}/SNR_{(control)}$) is inversely related to the strength of control responses. This finding is in accordance with the basic theory of SR in non-linear systems: weak signals (here sensory or postsynaptic

potentials) need a higher noise level (membrane potential fluctuations) to be pushed over the (spike) threshold than stronger signals (see also Pei *et al.*, 1996).

Background activity does not increase at high noise levels

The threshold-based SR theory also predicts that increasing noise should at some point lead to a purely noise (stimulus tremor)-induced activity increase. This should result in a strongly increased mean activity at higher tremor amplitudes and, as a consequence, the SNR would drop because stimulus-induced response peaks are submerged within the increased background activity. Opposite to this expectation, Fig. 5A shows that the mean rate of activity is actually decreased at higher stimulus tremor amplitudes. The solid curve in Fig. 5A shows the grand average of mean activity for all recordings obtained from the cell sample analysed above, the dashed lines give the standard deviation. Similar to the individual SNR functions (Fig. 3A, B and E), the grand average of the mean activity also shows a small (statistically insignificant) peak at low stimulus tremor amplitudes. More importantly at this point, however, is the observation that the mean activity declines steadily with increasing stimulus tremor. It clearly shows that the reduced SNR at higher stimulus tremor amplitudes cannot be attributed to an increase in purely noise-induced activity, instead it must result from a general decrease of responses when the tremor-induced noise gets too strong. This effect is also clearly visible in the examples of Figs 1 and 2, where the response peaks shrink above a certain stimulus tremor amplitude, accompanied with some broadening of the peaks, but with little tonic increase in activity as would be indicative of purely noise-induced activity. Accordingly, one can assume that even at high rates of mean activity, stimulus-driven response components dominate over purely noise-induced activity. This assumption is confirmed by the almost proportional increase in SNR despite increasing mean activity (Fig. 5B). A decline in SNR would be expected if background activity proportionally increases with increasing noise.

Large range of optimal noise level and relation to receptive field size

In total, we have found that about 80–85% of the 60 neurons tested showed a considerable increase in SNR (> 10%) with moderate stimulus tremor amplitudes (31 with motion, 20 with brightness modulation). For these cells, about 73% had a peak SNR at stimulus tremor amplitudes up to 0.2 deg, and even 40% were found in the smallest range of tremor (0.01–0.05 deg, Fig. 6B). In most cases, the SNR was almost doubled (see Fig. 4B). The question arises whether the optimal stimulus tremor amplitude might be related to the size of the receptive fields of the neurons. For the 53 cells for which we could reliably determine the diameter of the receptive field (width of on-subfield along bar motion trajectory), Fig. 6A shows that this assumption may hold only for a fraction of them, namely those scattered along the line with slope 1 (included in the dashed ellipse). The majority of cells shows a receptive field-invariant optimal stimulus tremor within the range of $\sigma = 0.01$–0.15 deg.

Quantification of SR effects by classical signal detection theory – ROC analysis

We also applied classical signal detection theory to our data by comparing the differences in interspike interval distributions for spontaneous and visually induced activity for records first obtained

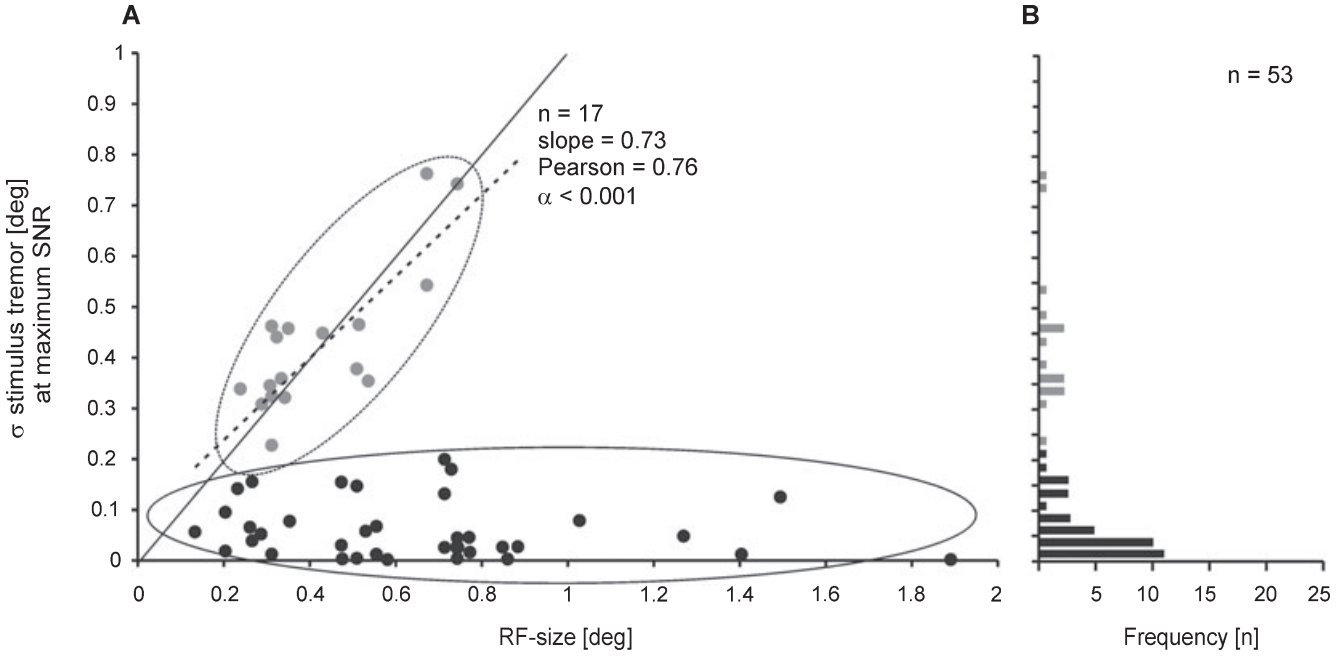

FIG. 6. Relationship between effective stimulus tremor level and receptive field size. (A) Stimulus tremor leading to maximal SNR is shown as a function of receptive field size. One group of data shows a correlation (ellipse including light grey dots), the other group does not (ellipse including black dots). The dashed line corresponds to the best linear regression for the 16 data points included in the dashed ellipse. The Pearson correlation coefficient (0.76) indicates a statistically significant correlation between stimulus tremor amplitude and receptive field size with $\alpha < 0.001$. (B) Distribution of optimal noise levels for inducing response improvement ($n = 53$, [34 motion, 19 brightness]). The grey level of bars corresponds to the grey level of dots in (A). RF, receptive field.

without stimulus tremor and then with different tremor amplitudes. To statistically quantify the difference between spike interval distributions, we calculated the ROC by plotting the number of correct hits (visual signal detected with signal present, corresponding to visually induced spike intervals) vs the number of false hits (visual signal detected without stimulus present, corresponding to spontaneous activity) for a criterion threshold sliding in 1 ms steps across the combined spike interval distributions (Fig. 7F, a). The AuROC is a quantitative measure for the degree of separation of the two interval distributions (see Fig. 7F, b). An area of 0.5 (normalized) would indicate totally overlapping distributions, an area of 1.0 would result if both distributions are completely separate. In a first step, we compared the interval distributions of spontaneous activity with the visually evoked activity, both without stimulus tremor (AuROC for the control situation). Then, those distributions obtained for the spontaneous activity evoked by a certain stimulus tremor amplitude but without a visual signal were compared with the activity evoked when both tremor and signal were combined (AuROC for noise). To quantify the effect of stimulus tremor on signal detection, we plotted the AuROC obtained with tremor relative to the normalized AuROC without tremor as a function of stimulus tremor amplitude (Fig. 7). In addition, we subdivided the data sample into five groups of different AuROC control level (Fig. 7A–E). We did this to test whether the effect of stimulus tremor also depends on the initial quality of signal detection without tremor, in analogy to the SNR in the former analysis (see Fig. 4). Interestingly, the stimulus tremor range inducing the strongest difference in spike interval distribution (0.01–0.5 deg) is almost identical to that for which a maximal increase of the SNR was found (see Fig. 6B). In accordance with SR theory, signal detection is improved only if it was originally weak (Fig. 7A and B). The percentage of cases with improved signal detection decreases from almost 100% (Fig. 7A) to less than 40% (Fig. 7E) within this tremor amplitude range with increasing initial (control, $AuROC_{contr}$) signal strength.

Discussion

Optimally balanced SR-like effect in cat visual cortex neurons

The results presented here demonstrate that visual noise caused by image jitter can improve the SNR of cortical visual responses. As is typical for SR, we found an improvement of the SNR for sub- and peri-threshold, but not for clearly supra-threshold visual stimuli. In addition, response improvement occurred only for weak noise levels [with the optimal noise level being inversely related to response strength (SNR) without noise], while higher noise levels somewhat diminished the SNR. This was evident for mean response amplitudes and SNR, as it was for signal detection quality based on spike interval distributions. Different from the classical concept of SR and also different from observations made for peripheral biological sensors (for review, see Moss *et al.*, 2004), a slight decrease in SNR at high noise levels was not related to increased neuronal background activity but resulted from a reduced visual response amplitude with marginally increased background activity, indicating a generally reduced responsiveness to visual inputs. Such behaviour is actually beneficial, as it prevents the cortical circuitry from being overloaded by useless activity while the specific visual activity is still of sufficient strength and the SNR is little affected. What could be the reason for the reduction of noised-induced background activity? We assume that the characteristics of cortical sensory processing are most suitable to achieve this. First, cortical cells show stronger temporal low-pass filter characteristics for brightness dynamics than the peripheral sensory neurons (Movshon, 1975), therefore responding less to the faster rate of change in brightness associated with increased noise amplitudes. A second, more powerful mechanism of active noise suppression may evolve from the cortical pattern of connectivity, with long-range lateral projections and inhibitory feedback loops. Noisy background activity may be 'normalized' in a similar way as discussed for activity resembling contrast adaptation (Ohzawa *et al.*, 1982; Heeger, 1992; Carandini *et al.*, 1999) and contrast-invariant orientation tuning (Anderson *et al.*, 2000). As recently proposed by Wenning & Obermayer (2003), such an adaptive process may happen even at the level of a single cortical neuron via an intrinsic feedback mechanism. The process they call 'activity-driven adaptive stochastic resonance' regulates the synaptic weight of noisy inputs in dependence on the average spike output activity of the neuron. Because the average output level of the neuron does not allow distinguishing between inputs related to noise and those elicited by the visual stimulus itself, both noise activities and stimulus-driven activities will be scaled down to the same degree at increasing output rates, just what we observed in our recordings. Another consequence of such an adaptive process would be that a certain small noise level is actually needed to prevent neurons from getting supersensitive during the absence of specific inputs. Ongoing afferent noise would keep neurons at a similar adaptive level.

Methodical limitations

This study was intended to test whether cortical neurons, which receive strong convergence of cortical inputs in addition to the bottom-up afferent pathway, may still benefit from an SR effect assumed to appear primarily at the retinal level. Therefore, we kept the spatial characteristics of visual stimuli (bar size) constant and only adapted the dynamic aspects (motion amplitude, brightness modulation amplitude) to individual cortical neurons to achieve peri-threshold, little supra-threshold and clearly supra-threshold responses. Therefore, the width of the bar stimulus was not adapted to the width of the receptive field of cortical neurons. As a compromise, we set the bar width to 0.25 deg, a width within the range of central retinal receptive field diameters and just sufficiently large to elicit weak cortical responses. As a consequence, the bar might cover the complete receptive field of some cells but only a fraction of the receptive field of other cells. Although this might primarily affect the neuronal response strength (which was counterbalanced by stimulus-amplitude modulation), it cannot be excluded that addition of noise may be differently effective. However, only a small fraction of cortical receptive fields ($n = 5$, corresponding to 9%) were estimated to be somewhat smaller than the width of the stimulus, so that the effect of bar width may be neglected for the whole population. With large stimulus tremor amplitudes, the stimulus would also transiently leave the receptive field. However, this cannot be an explanation for the reduced activity observed with higher noise amplitudes as discussed above. Because cortical cells (and also photoreceptors) respond better to transients than to steady stimuli, a bright stimulus completely leaving the receptive on-field and returning to it would be a stronger stimulus than a stimulus permanently covering parts of the on-field. In the same way, larger amplitudes for the sinusoidal bar motion led to stronger responses than small-amplitude motion even when the stimulus had left the receptive field.

A second aspect to be discussed is the characteristics of the noise. In our experiments, the frequency range to jitter the visual image was not adapted to a certain type of eye movement (e.g. microtremor of 30–65 Hz in cat), but covered a broad range up to 200 Hz. This was

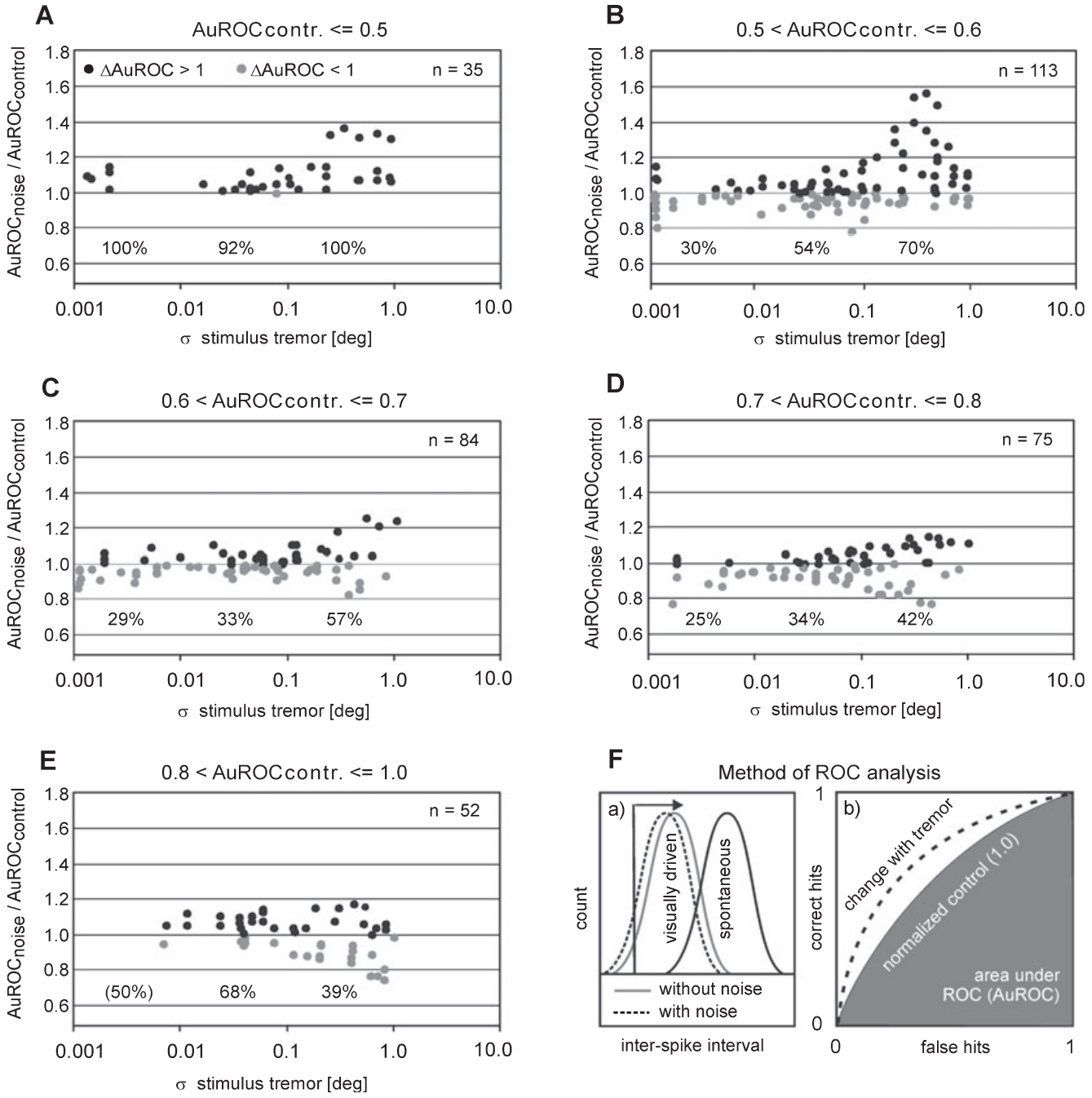

FIG. 7. Signal detection theory analysed with receiver operator characteristic (ROC). (A–E) The relative changes in area under the ROC curve ($AuROC_{noise}/AuROC_{control}$) as a function of stimulus tremor added to the visual signal. As schematically illustrated in (F), AuROC was calculated separately for the stimulus condition without stimulus tremor (comparison of the distribution of spontaneous and visually driven interspike intervals with ROC, see hypothetized spike-interval distributions in (Fa) *and* the grey area in (Fb), and for the stimulus situation with stimulus tremor applied, see dashed lines in (Fa) and (Fb). The ROC curve in (Fb) is established by moving the criterion threshold, the vertical bar in (Fa), from left to right while plotting the area of one interval distribution (for visual activity), which is already left to the bar vs the area of the other distribution (for spontaneous activity), which is left to the bar. If both distributions would be identical, the ROC curve would be a straight line with a slope of 1 and the relative area below it (AuROC) would be 0.5 of the total possible area. Assuming that visual stimulation increases neuronal activity above the spontaneous activity level (decreasing interspike intervals and shifting the distribution to the left, Fa), AuROC values can be expected to lie in the range of 0.5 (total overlap of both distributions) to 1.0 (total separation of the distributions). The larger the AuROC, the better the separation of correct signals from background activity. (A–E) Changes in AuROC achieved by adding stimulus tremor are given relative to normalized AuROC without tremor (control, $AuROC_{contr}$) and plotted vs standard deviation (σ) of stimulus tremor amplitude. Subdividing the data according to $AuROC_{contr}$ (A–E) shows that stimulus tremor with a σ value of 0.1–0.5 improves signal detection only if the signal without tremor is originally weak (A and B). Percentage values at the bottom of diagrams indicate the relative number of cases with improved signal detection (> 1.0, black dots vs < 1.0, grey dots) due to stimulus tremor within the corresponding magnitude order. Data for moving and brightness-modulated bars are pooled.

done to consider all possible frequency components generated by the different eye movements found during fixation (microtremor, microsaccades and slow drifts). Because eye movements do not follow a sinusoidal space–time relationship but are usually jerk-like, the upper limit of potentially relevant frequencies is clearly higher than the periodicity at which the movements occur. With regard to other findings of SR effects on neuronal activity (see Moss *et al.*, 2004), we assume that frequencies within the upper range (30–100 Hz) are most suitable to carry the SR effect also for cortically evoked activity (see also below), and that a band-passed noise (e.g. 30–65 Hz) will yield similar effects.

Possible contribution of eye movements to the SR effect

The majority of cortical cells showed an optimal stimulus tremor amplitude within the range of 0.01–0.15 deg. This resembles the upper range of eye microtremor amplitudes in humans and cats (which are generated at a frequency of 30–150 Hz in humans, Carpenter, 1988; Bolger *et al.*, 1999; at 30–65 Hz in cats, Pritchard & Heron, 1960; Hebbard & Marg, 1960), and corresponds to a retinal distance of 3–45 μm. Considering the threefold larger photoreceptor spacing in cat central retina compared with humans (Steinberg *et al.*, 1973; Wässle & Boycott, 1991), a contrast edge jittered with this amplitude would maximally stimulate three neighbouring photoreceptors in cat retina. An SR effect induced within this noise amplitude range could thus be assumed to be primarily of retinal origin. Those cells showing an optimal amplitude scaling with RF size indicate that a second SR effect may result form the convergence and integration of afferent inputs transmitting synchronous noise activity. Given the supposed hierarchy of simple to complex cell input (Martinez & Alonso, 2001), this effect might be stronger in complex cells. We did not distinguish between simple and complex cells, but focused on cells showing spatially well-circumscribed RF subunits to allow proper placement of the visual stimulus. This might have biased the sample towards simple cells, although some complex cells show small receptive field subunits too (Martinez *et al.*, 2005). A proper distinction between simple and complex cells would require receptive field tests with bright and dark stimuli, or the presentation of moving gratings for testing linearity of spatial contrast integration, which was not possible with our setup. Thus, it cannot be excluded that the larger group of cells showing receptive field size-independent best noise level belong to the simple fraction, while those cells showing receptive field size dependence are of the complex type.

One can further ask what are the characteristics of noise that may optimally support signal processing in the nervous system, and if a particular source of noise may be more advantageous than others. To support the process of SR, the noise should include frequency components that are a few times higher than the frequencies by which stimulus aspects change. Membrane potential fluctuations within the gamma frequency range (30–100 Hz) have been demonstrated to be suitable to improve orientation and direction selectivity (Volgushev *et al.*, 2003), and contrast invariance of orientation tuning (Anderson *et al.*, 2000). Noise within this frequency range is discussed to evolve from the multiple synaptic interactions within the cortical network, but one can further assume that noise generated in the periphery and transmitted to the cortex by sensory afferents could induce these frequencies equally well. Actually, tremor-like eye movements cover almost the same frequency range as gamma activity (30–65 Hz in cat, Hebbard & Marg, 1960; Pritchard & Heron, 1960; 30–150 Hz in humans, Carpenter, 1988; Bolger *et al.*, 1999), and would induce a noise pattern ideally suited to support SR-like processes. However, there is one principal difference between noise induced peripherally by small eye movements and noise generated centrally by synaptic interactions: while synaptic interactions will primarily induce spatially stochastic activity and a synchronous pattern of activity only within a subset of neurons, eye movement will cause a globally synchronous pattern of noise activity within the afferent pathway and cortex. This may be of advantage for processes concerned with the final elimination of noise at later stages of processing. Either a synchronous discharge volley due to stimulus jitter or a discharge volley originating from oculomotor commands (efference copy) may be able to prevent image jitter to reach perceptional levels as discussed for saccadic eye movements (Diamond *et al.*, 2000; Thiele *et al.*, 2002).

Final conclusions

We demonstrate that noise induced by jittering the visual image within a frequency and amplitude range covering the range of small eye movements enhanced the detection of peri-threshold visual signals by neurons in cat primary visual cortex via a process similar to SR. However, different from typical SR behaviour, cortical cells do not show a noisy background activity that proportionally increases with input noise. Cortical cells seem to optimize the SR effect by adjusting their response gain to the noisy input. Thereby, they take the benefit of noise-enhanced signal detection for weak stimuli and keep the SNR of sensory activity high at increasing noise levels.

Acknowledgements

This work was supported by grants (SFB 509, A2 and A4) to K.F. and F.W. of the Deutsche Forschungsgemeinschaft (DFG) as well as the European Commission (DRIVSCO, F.W.). In addition, the support of the BMBF, BCCN-Goettingen, TP-W3 is gratefully acknowledged. We like to thank D. Winkler and Y. Zhao for technical assistance, B. Li and M. Volgushev for comments on the manuscript, and U.T. Eysel for logistic and intellectual support as well as for his helpful comments.

Abbreviations

ACF, auto-correlation function; AP, action potential; AuROC, area under ROC curve; EEG, electroencephalogram; LED, light-emitting diode; PSTH, peri-stimulus time histogram; ROC, receiver operator characteristics; SNR, signal-to-noise ratio; SR, stochastic resonance.

References

Anderson, J.S., Lampl, I., Gillespie, D.C. & Ferster, D. (2000) The contribution of noise to contrast invariance of orientation tuning in cat visual cortex. *Science*, **290**, 1968–1972.

Bolger, C., Bojanic, S., Sheahan, N.F., Coakley, D. & Malone, J.F. (1999) Dominant frequency content of ocular microtremor from normal subjects. *Vis. Res.*, **39**, 1911–1915.

Carandini, M., Heeger, D.J. & Movshon, J.A. (1999) Linearity and gain control in V1 simple cells. In Ulinski, P.S., Jones, E.G. & Peters, A. (Eds), *Cerebral Cortex, Vol. 13: Models of Cortical Function*. Kluwer Academic, New York, pp. 401–443.

Carpenter, R.H.S. (1988) *Movements of the Eyes*, 2nd Edn. Pion, London.

Collins, J.J., Imhoff, T.T. & Grigg, P. (1996a) Noise-enhanced information transmission in rat SA1 cutaneous mechanoreceptors via aperiodic stochastic resonance. *J. Neurophysiol.*, **76**, 642–645.

Collins, J.J., Imhoff, T.T. & Grigg, P. (1996b) Noise-enhanced tactile sensation. *Nature*, **383**, 770.

Cordo, P., Inglis, J.T., Verschueren, S., Collins, J.J., Merfeld, D.M., Rosenblum, S., Buckley, S. & Moss, F. (1996) Noise in human muscle spindles. *Nature*, **383**, 769–770.

Diamond, M.R., Ross, J. & Morrone, M.C. (2000) Extraretinal control of saccadic suppression. *J. Neurosci.*, **20**, 3449–3455.

Ditzinger, T., Stadler, M., Struber, D. & Kelso, J.A. (2000) Noise improves three-dimensional perception: stochastic resonance and other impacts of noise to the perception of autostereograms. *Phys. Rev. E. Stat. Phys. Plasma Fluids Relat. Interdiscipl. Topics*, **62**, 2566–2575.

Douglass, J.K., Wilkens, L.A., Pantazelou, E. & Moss, F. (1993) Noise enhancement of information transfer in crayfish mechanoreceptors by stochastic resonance. *Nature*, **365**, 337–340.

Greschner, M., Bongard, M., Rujan, P. & Ammermüller, J. (2002) Retinal ganglion cell synchronization by fixational eye movements improves feature estimation. *Nat. Neurosci.*, **5**, 341–347.

Hebbard, F.W. & Marg, E. (1960) Physiological nystagmus in the cat. *J. Opt. Soc. Am.*, **50**, 151–155.

Heeger, D.J. (1992) Normalization of cell responses in cat striate cortex. *Vis. Neurosci.*, **9**, 181–197.

Ikeda, H. & Wright, M. (1974) Sensitivity of neurones in visual cortex (area 17) under different levels of anesthesia. *Exp. Brain Res.*, **20**, 471–484.

Levin, J.E. & Miller, J.P. (1996) Broadband neural encoding in the cricket cercal sensory system enhanced by stochastic resonance. *Nature*, **380**, 165–168.

Li, B., Funke, K., Wöergötter, F. & Eysel, U.T. (1999) Correlated variations in EEG pattern and visual responsiveness of cat lateral geniculate relay cells. *J. Physiol. (Lond.)*, **514.3**, 857–874.

Manjarrez, E., Diez-Martinez, O., Mendez, I. & Flores, A. (2002) Stochastic resonance in human electroencephalographic activity elicited by mechanical tactile stimuli. *Neurosci. Lett.*, **324**, 213–216.

Martinez, L.M. & Alonso, J.M. (2001) Construction of complex receptive fields in cat primary visual cortex. *Neuron*, **32**, 515–525.

Martinez, L.M., Wang, Q., Reid, R.C., Pillai, C., Alonso, J.M., Sommer, F.T. & Hirsch, J.A. (2005) Receptive field structure varies with layer in the primary visual cortex. *Nat. Neurosci.*, **8**, 372–379.

Moliadze, V., Giannikopoulos, D.V., Eysel, U.T. & Funke, K. (2005) Paired-pulse TMS protocol applied to visual cortex of anaesthetised cat: effects on visually evoked single unit activity. *J. Physiol. (Lond.)*, **566**, 955–965.

Mori, T. & Kai, S. (2002) Noise-induced entrainment and stochastic resonance in human brain waves. *Phys. Rev. Lett.*, **88**, 218101.

Moss, F., Ward, L.M. & Sannita, W.G. (2004) Stochastic resonance and sensory information processing: a tutorial and review of application. *Clin. Neurophysiol.*, **115**, 267–281.

Movshon, J.A. (1975) The velocity tuning of single units in cat striate cortex. *J. Physiol. (Lond.)*, **249**, 445–468.

Ohzawa, I., Sclar, G. & Freeman, R.D. (1982) Contrast gain control in the cat visual cortex. *Nature*, **298**, 266–268.

Osaka, T., Yamashita, H. & Kannan, H. (1988) A nonlinear amplifier for improving signal-to-noise ratio of single unit recordings. *Brain Res. Bull.*, **21**, 143–145.

Pei, X., Wilkens, L. & Moss, F. (1996) Noise-mediated spike timing precision from aperiodic stimuli in an array of Hodgekin-Huxley-type neurons. *Phys. Rev. Lett.*, **77**, 4679–4682.

Priplata, A., Niemi, J., Salen, M., Harry, J., Lipsitz, L.A. & Collins, J.J. (2002) Noise-enhanced human balance control. *Phys. Rev. Lett.*, **89**, 238101.

Pritchard, R.M. & Heron, W. (1960) Small eye movements of the cat. *J. Psychol.*, **14**, 131–137.

Simonotto, E., Riani, M., Seife, C., Roberts, M., Twitty, J. & Moss, F. (1997) Visual perception of stochastic resonance. *Phys. Rev. Lett.*, **78**, 1186–1189.

Steinberg, R., Reid, M. & Lacy, P. (1973) The distribution of rods and cones in the retina of the cat (Felis domesticus). *J. Comp. Neurol.*, **148**, 229–248.

Thiele, A., Henning, P., Kubischik, M. & Hoffmann, K.-P. (2002) Neural mechanisms of saccadic suppression. *Science*, **295**, 2460–2462.

Volgushev, M., Pernberg, J. & Eysel, U.T. (2003) Gamma-frequency fluctuations of the membrane potential and response selectivity in visual cortical neurons. *Eur. J. Neurosci.*, **17**, 1768–1776.

Wässle, H. & Boycott, B. (1991) Functional architecture of the mammalian retina. *Physiol. Rev.*, **71**, 447–479.

Wenning, G. & Obermayer, K. (2003) Activity driven adaptive stochastic resonance. *Phys. Rev. Lett.*, **90**, 120602–120601.